

An alternative methodology for the analysis of electrical resistivity data from a soil gas study

Sara Johansson^{1,2}, Håkan Rosqvist³, Mats Svensson², Torleif Dahlin⁴
and Virginie Leroux⁴

¹Department of Physics, Lund University, Lund, Sweden. E-mail: scwsp@mahidol.ac.th

²Tyréns AB, Malmö, Sweden

³NSR AB, Helsingborg, Sweden

⁴Engineering Geology, Lund University, Lund, Sweden

Accepted 2011 May 13. Received 2011 May 13; in original form 2010 February 26

SUMMARY

The aim of this paper is to present an alternative method for the analysis of resistivity data. The methodology was developed during a study to evaluate if electrical resistivity can be used as a tool for analysing subsurface gas dynamics and gas emissions from landfills. The main assumption of this study was that variations in time of resistivity data correspond to variations in the relative amount of gas and water in the soil pores. Field measurements of electrical resistivity, static chamber gas flux and weather data were collected at a landfill in Helsingborg, Sweden. The resistivity survey arrangement consisted of nine lines each with 21 electrodes in an investigation area of 16 × 20 m. The ABEM Lund Imaging System provided vertical and horizontal resistivity profiles every second hour. The data were inverted in Res3Dinv using L₁-norm-based optimization method with a standard least-squares formulation. Each horizontal soil layer was then represented as a linear interpolated raster model. Different areas underneath the gas flux measurement points were defined in the resistivity model of the uppermost soil layer, and the vertical extension of the zones could be followed at greater depths in deeper layer models. The average resistivity values of the defined areas were calculated and plotted on a time axis, to provide graphs of the variation in resistivity with time in a specific section of the ground. Residual variation of resistivity was calculated by subtracting the resistivity variations caused by the diurnal temperature variations from the measured resistivity data. The resulting residual resistivity graphs were compared with field data of soil moisture, precipitation, soil temperature and methane flux. The results of the study were qualitative, but promising indications of relationships between electrical resistivity and variations in the relative amount of gas and water in the soil pores were found. Even though more research and better data quality is necessary for verification of the results presented here, we conclude that this alternative methodology of working with resistivity data seems to be a valuable and flexible tool for this application.

Key words: Time series analysis; Numerical approximations and analysis; Electrical properties; Hydrogeophysics; Permeability and porosity; Equations of state.

INTRODUCTION

In landfill research, electrical resistivity measurements are particularly suitable for detecting leachate, because of the large decrease in resistivity these features create. The idea of using resistivity for detecting subsurface gas or estimating gas emissions is relatively new.

During 2007, a field investigation at the Filborna landfill outside Helsingborg in Sweden was carried out. The aim was to use time-lapse electrical resistivity monitoring to follow water migration during and after leachate recirculation. An unexpected result

was that irregular zones of increased resistivity occurred at various locations during the experimental period. These zones were interpreted as possible subsurface gas accumulations (Rosqvist *et al.* 2007). The idea of interpreting high-resistivity zones in landfills as gas accumulations was also presented by Moreau *et al.* (2004). Their investigation site was located at a French bioreactor, where relative changes in resistivity were studied during a leachate recirculation event. In one part of the landfill, the electrical resistivity first decreased, after which it increased before returning to the initial value. Another zone showed the opposite behaviour with an initial rise of resistivity followed by a decrease, before returning

to the reference value. The interpretation of this pattern was that a simultaneous flow of both liquid and gas in the concerned porous areas could cause the observed variations in resistivity (Moreau *et al.* 2004).

The two main gas transport mechanisms in soils are diffusion and advection. Diffusion is a molecular transport process driven by a concentration gradient, whereas advection involves movements of whole air volumes due to pressure imbalances (Barber *et al.* 1990; Campbell 1998; Stepniewski *et al.* 2002). Even though the processes involved in soil gas transport inside landfills are known, large uncertainties regarding the actual pattern of subsurface gas movements still remain. This causes a problem, especially in landfill gas models. The uncertainties originate in the structural heterogeneity of landfills; differences in waste composition and density create large variations in porosity, soil moisture and hydraulic conductivity across a landfill that are difficult to model without exhaustive excavations (Crawford & Smith 1985; Lamborn 2007). The heterogeneity of landfill soils also results in highly variable spatial and temporal patterns of gas emissions from landfills (approximately 55 per cent methane, CH₄ and 45 per cent carbon dioxide, CO₂; Crawford & Smith 1985).

The interpretation from the earlier studies of noticeably increased resistivity in various landfill zones as gas accumulations has not yet been verified. Another possibility is that the zones could be the result of inversion artefacts. The latter was discussed at the 'Workshop on 'Geophysical measurements at landfills' in Malmö, 2008. However, during 2008 a project that aimed to investigate the possibilities of detecting and verifying gas accumulations in landfills with electrical resistivity was carried out (Rosqvist *et al.* 2009). One of the objectives was to evaluate if resistivity data can be useful as a tool for studies of subsurface gas dynamics, and linked to the varying gas emissions from landfill soil surfaces (Johansson 2009). It was to address this question that the field measurements and data analysis presented in this paper were performed.

The aim of this paper is to present the methodology of the resistivity data analysis, together with results focused around one of six selected field measurement points. For a more detailed description of the project as a whole, see Rosqvist *et al.* (2009) and Johansson (2009).

MATERIAL AND METHODS

Data collection

The field investigation was carried out during the summer of 2008 at the Filborna landfill in Helsingborg, Sweden. An investigation area of 16 × 20 m was chosen on the top of an uncovered deposition cell. The waste in the uppermost 0.0- to 0.5-m-thick soil layer was more than 60 years old and did not produce gas anymore, whereas more recent, gas-producing material was deposited further down.

Electrical resistivity was systematically measured with the ABEM Lund Imaging System, an automatic system that provided a full resistivity data set every second hour during June to September 2008. The survey arrangement consisted of nine electrode lines with 21 electrodes each. The electrode spacing was 1 m and the distance between each pair of lines was 2 m. Relatively small spacings between the electrodes and the lines were chosen to obtain high spatial resolution. The pole-dipole array in forward and reverse configurations was used for the measurements to obtain deep ground penetration, and the distant electrode was located approximately 100 m away from the measurement area.

A weather station with a Campbell C1000 data logger (Campbell Manufacturing) recorded soil temperature at 5-cm depth below the soil surface and precipitation (ARG10, tipping bucket) every second in the immediate vicinity of the investigation area. The weather station logger sometimes underestimated the amount of precipitation, but reliably recorded the times of all rain events. In addition, twelve 30-cm-long time domain reflectometer (TDR)-probes were installed in the ground, equally spaced over a large part of the investigation area. The TDR-probes were connected to a multiplexer and a TDR100-instrument, and the measurements were made manually and concurrent with gas flux measurements. Soil moisture values were calculated with the response curves from the TDR-instrument, but unfortunately the magnitude of the values turned out to be rather uncertain, mainly because no soil samples needed for calibration of the TDR-probes were collected at the site.

Measurements of CH₄ flux from the soil surface were made with the static chamber method during five field days (August 18–22). The principal concept of the method is to measure how the concentration of a specific gas rises inside a chamber, placed upon a gas-emitting surface. Three air samples were collected with syringes from the chambers during each measurement. The chambers, which occupied 0.055 m² areas of the ground when placed on the soil surface, were sealed to the ground with clay to prevent air leakage. Six fixed measurement points in the investigation area were selected for the static chamber measurements (Fig. 1). Three of the measurement points were located over zones with relatively high resistivity values (points K1, K2 and K3) and the other three over zones with lower resistivity values (points K4, K5 and K6). The measurements were carried out between one and three times a day at all measurement points. In the laboratory, the concentration of CH₄ in the air samples was analysed through separation by gas chromatography (GC, Shimadzu 17A) and detection by flame ionization detection (FID). Injection/detection and column oven temperatures were 140 and 70 °C, respectively. The samples were introduced into the GC column (Porapak Q) by syringe injection via a 1 mL sample loop. Helium was used as the carrier gas with a flow rate of 40 mL min⁻¹. The CH₄ fluxes (mg CH₄ m⁻² hr⁻¹) were calculated on the basis of the linear change in chamber concentration with time.

Data analysis

The resistivity data for each set of measurements were inverted in Res3Dinv (Geotomo Software Sdn, Bhd; Loke 2008), using L₁-norm-based optimization method with a standard least squares formulation. Because the L₁-norm minimizes the sum of the absolute values of the data misfit, the effect of bad data points is reduced compared with the standard least squares (L₂) optimization method (Loke *et al.* 2003). A 3D-model was computed for each time a measurement was taken with the same constraints and the same grid geometry each time. The total number of cells in the model was 10 880, and the dimensions of each cell corresponded to $x = 0.5$ m, $y = 1.0$ m and $z_1 = 0.224$ m, $z_2 = 0.260$ m and $z_3 = 0.296$ m in layers 1, 2 and 3, respectively. As the ground surface was essentially flat, topography was not incorporated in the models. A homogeneous half-space based on the average of the logarithms of the measured apparent resistivities was used as starting model for the inversions. Because the available version of the software did not support time-lapse inversion, each data set was inverted individually and the difference between the time steps and various statistical parameters were calculated afterwards.

The measured data were generally of high quality illustrated by small residuals and the smooth appearance of the measured data.

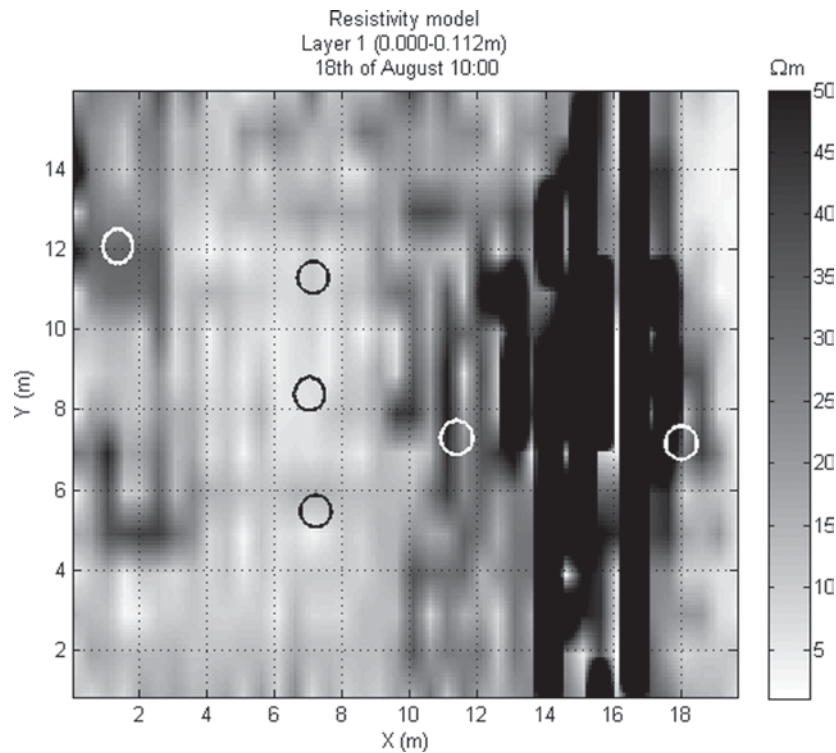


Figure 1. The location of the CH₄ flux measurement points on a horizontal resistivity profile from the initial day of the investigation period. All zones with resistivity values exceeding 50 Ωm are shown in black. The white circles marks measurement points K1, K3 and K2 (left to right) and the black circles K6, K5 and K4 (down from above).

The number of measurement points used in the inversions of the data sets from 10:00 on August 18 to 12:00 on August 22 was nearly always 3888, with a few exceptions of 3885–3887 measurement points. The residual error of the inversions during the same period was 4.5 ± 0.2 per cent. From the period 14:00 to 22:00 on August 22, the data quality was slightly worse. The number of measurement points was 3860, and the residual error 7.2 ± 0.1 per cent.

The inverted resistivity data consisted of 640 coordinate values in each horizontal resistivity layer (in total 17 layers). The inverted data for each layer and each model were plotted as raster images, but the resolution was too rough for a spatial analysis. The flux measurements were representative for 0.055 m² circular areas of the soil (occupied by the chambers), whereas each cell in the resistivity models corresponded to a 0.5 m × 1.0 m area of the soil. The difference in resistivity between neighbouring cells was often large as a consequence of the low spatial resolution of the model. To smooth the data values and to obtain a more realistic representation of the soil, the resistivity model was linearly interpolated. Each cell in the interpolated model then corresponded to a 0.1 m × 0.1 m area of the soil. The main reason for the linear interpolation was to decrease the size of the model cells to be able to select areas (each containing several interpolated model cells) underneath the gas measurement positions. An average of the resistivity values in each defined area was calculated for each resistivity measurement. One benefit of using linear interpolation was that the resistivity values of not only the closest model cell, but also the surrounding model cells were taken into consideration in the analysis. Taking more than one inverted data value into account reduces the uncertainty in the data analysis.

It was noticed early on from a visual interpretation that zones of high resistivity values seemed to vary between growing larger and smaller over time. Apart from that, there was no dramatic temporal change in the overall resistivity distribution of the investigation area.

Underneath measurement points K1, K2 and K3 definitions of high-resistivity zones were made by identifying borders around the zones where the resistivity values dropped rapidly. It was possible to follow the vertical extension of the defined areas by comparing the horizontal resistivity profiles of different depths (Fig. 2a–c). In layer 4 (0.6–1.0 m), the resolution of the resistivity data had decreased so much that it became difficult to follow the defined areas at greater depths. The soil layers below layer 3 (0.4–0.6 m) were therefore left out of the analysis. The resistivity values underneath measurement points K4, K5 and K6 were low over a large area, with no steep changes in resistivity. At these locations, rectangular areas corresponding to 0.33 m² of the soil surrounding the chambers were selected in the resistivity model to represent the soil below the measurement points.

Data collected every 2 hr from August 18 10:00 to August 22 22:00 were used in the data analysis. The average resistivity values in the defined areas were calculated for each time step and plotted on a time axis. The number of model cells included in each area corresponding to the measurement points was defined by the data from the first time step, and the definitions of the areas were thereafter kept constant irrespective of the development of the values in the included and surrounding model cells. Because of the relatively large time step in the resistivity data, the graphs of resistivity variations over time were interpolated with quadratic splines to get a continuous representation of the variations (Fig. 3).

The graphs showing the variations in resistivity over time are likely to reflect changes of the soil state in the defined areas throughout the investigated period. All soils consists of mineral particles (geological or organic), water and gas. The relative ratios of these constituents can be described by the following relationship:

$$\phi = \alpha + \theta = 1 - \frac{\rho_b}{\rho_m}, \quad (1)$$

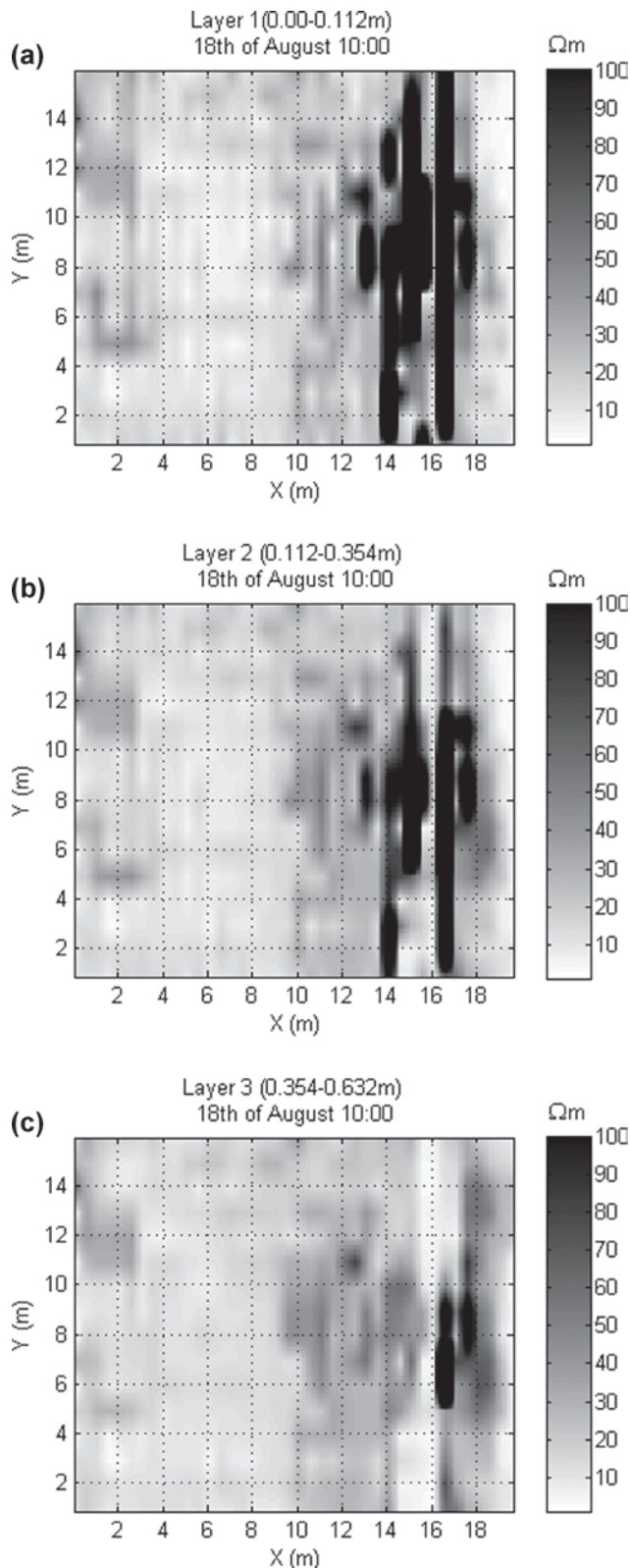


Figure 2. Horizontal resistivity models showing zones with resistivity values exceeding $100 \Omega\text{m}$ in black. (a) The limitations of a possible gas accumulation below measurement point K2 could be distinguished in layer 1 (0.0–0.1 m) of the soil (compare with Fig. 1) and followed into (b) layer 2 (0.1–0.4 m) and (c) layer 3 (0.4–0.6 m).

where ϕ is the total soil porosity, α is the volumetric air content and θ is the volumetric water content of the pores. The bulk density ρ_b is the total density of the dry soil, whereas ρ_m represents the density of the mineral soil particles (Chapin 2002; Tang 2003). Since 5 days is a relatively short period of investigation, settlement of the landfill and other possible causes of physical changes in the ground can be neglected. With a constant pore volume, the variations in soil state reflected by resistivity logically depend on the relative amount of gas and water contained in the soil pores. It is presumed that decreasing resistivity corresponds to an increased amount of water in the soil pores and vice versa.

However, before any reliable attempt to interpret the variations in resistivity could be made, the influence of the varying soil temperature on the measured resistivity values had to be taken into consideration. Soil temperature has an effect on resistivity, because the conductivity of materials increases with increasing temperatures. The temperature effect on resistivity measurements follows the well-known equation:

$$\rho_t = \frac{\rho_r}{1 + \alpha(t - t_r)}, \quad (2)$$

where ρ_r is the resistivity measured at a reference temperature t_r , t is the ambient soil temperature and α is the temperature coefficient of resistivity which has an approximate value of 0.025 per degree (Keller *et al.* 1966).

The temperature effect in eq. (2) has nothing to do with the physical amount of gas or water in the soil pores, but only the mobility of the ions present in the soil. Therefore, this effect was modelled from the soil temperature data measured at the field site and subtracted from the measured resistivity values (Fig. 3). In this way, graphs showing the *residual variation in resistivity* could be produced. The residual variation in resistivity could only be calculated for the uppermost soil layer (layer 1, 0.0–0.1 m), because soil temperature was not measured at deeper depths. However, the diurnal variations in soil temperature decrease rapidly with depth, which means that the temperature effect on resistivity is less significant in the deeper layers.

This method leads to the assumption that the main variations in the residual resistivity graphs correspond to a change in the relative amount of gas and water in the soil pores, because the temperatures effect on resistivity has been removed from the graphs.

The residual variations in resistivity were compared with the gas flux data as well as the meteorological data collected in field, to evaluate whether or not the variations seen in the resistivity data were likely to reflect physical changes in the soil.

RESULTS

Measurement point K2 showed what was considered the most interesting results of all six measurement points during the investigation period. The reason for this is related to the high variability in resistivity ($\sim 50 \Omega\text{m}$ in 1 week). Point K2 was located in a zone of particularly high resistivity values (possibly a gas accumulation) with values that ranged from 100 to $150 \Omega\text{m}$ in the uppermost soil. In Fig. 4, the measured resistivity variations in soil layers 1, 2 and 3 below measurement point K2 are plotted together with the CH_4 fluxes measured at the soil surface. It can be seen that the resistivity is generally higher in layer 2 than in layer 1, but that the layers exhibited similar behaviour. In other words, when the resistivity increases in layer 1, it also increases in layer 2 but not necessarily by the same amount. However, in layer 3 the variations differ, and sometimes even behave opposite to the upper soil (compare for

Figure 3. Comparison between the measured resistivity variations (layer 1 at point K2) and the variations that would be theoretically expected from the variations in soil temperature alone.

Figure 4. CH₄ fluxes from the soil surface at measurement point K2, and the measured variations in resistivity in soil layers 1–3.

example the negative peaks in layers 1 and 2 with the simultaneous positive peak in layer 3 at 22:00 on August 19).

Fig. 5(a) below shows the residual variation in resistivity of layer 1 together with CH₄ fluxes from measurement point K2. A comparison of Figs 4 and 5(a) stresses how the graphs of residual variation in resistivity helps to differentiate between physical changes in the soil and variations caused by temperature variations. In contrast to the original inverted data in Fig. 4, three major resistivity peaks and a clearly decreasing trend of resistivity during the investigation period can be observed in Fig. 5(a).

Fig. 5(b) shows the precipitation and soil moisture data throughout the investigation period. Three larger rain events during the first